Creation of a blood-compatible surface: a novel strategy for suppressing blood activation and coagulation using nitroxide radical-containing polymer with reactive oxygen species scavenging activity

Toru Yoshitomi[a], Yu Yamaguchi[a], Akihiko Kikuchi[b] and *Yukio Nagasaki[a,c-d]

[a] Graduate School of Pure and Applied Sciences, University of Tsukuba, Tennoudai 1-1-1, Tsukuba, Ibaraki, 305-8573, Japan

[b] Department of Materials Science and Technology, Tokyo University of Science, Yamazaki 2641, Noda, Chiba, 278-8510, Japan

[c] Master's School of Medical Sciences, Graduate School of Comprehensive Human Sciences, University of Tsukuba, Tennoudai 1-1-1, Tsukuba, Ibaraki, 305-8573, Japan

[d] Satellite Laboratory, International Center for Materials Nanoarchitectonics (MANA), National Institute for Materials Science (NIMS), University of Tsukuba, Tennoudai 1-1-1, Tsukuba, Ibaraki, 305-8573, Japan

*Corresponding author: Prof. Yukio Nagasaki, Graduate School of Pure and Applied Sciences, Master's School of Medical Sciences, Graduate School of Comprehensive

Human Sciences, Satellite Laboratory, International Center for Materials

Nanoarchitectonics (MANA), National Institute for Materials Science (NIMS),

University of Tsukuba, Tennoudai 1-1-1, Tsukuba, Ibaraki, 305-8573, Japan

Phone: +81-29-853-5749

Fax: +81-29-853-5749

E-mail information: yukio@nagalabo.jp

ABSTRACT

Various polymeric materials have been used in medical devices, including blood-contacting artificial organs.   Contact between blood and foreign materials causes blood cell activation and adhesion, followed by blood coagulation.   Concurrently, the activated blood cells release inflammatory cytokines together with reactive oxygen species (ROS).   We have hypothesized that the suppression of ROS generation plays a crucial role in blood activation and coagulation.   To confirm this hypothesis, surface-coated polymers containing nitroxide radical compounds (nitroxide radical-containing polymer; NRP) were designed and developed.   The NRP was composed of a hydrophobic poly(chloromethylstyrene) (PCMS) chain in which 2,2,6,6-tetramethylpiperidine-N-oxyl   (TEMPO)   moieties   were   conjugated   via condensation reaction of the chloromethyl groups in PCMS with the sodium alkolate group of 4-hydroxy-TEMPO.   Blood compatibility was investigated by placing NRP-coated beads in contact with rat whole blood.   The amount of ROS generated on PCMS-coated beads used as a control increased significantly with time, while NRP-coated beads suppressed ROS generation.   It is interesting to note that the suppression of inflammatory cytokine generation by NRP-coated beads was shown to be significantly higher than that of PCMS-coated beads.   Both platelet and leukocyte

adhesions on the beads were suppressed with increasing extent of the TEMPO component in the polymer.   From these results, it is confirmed that the suppression of ROS by NRP prevents inflammatory cytokine generation, which in turn results in the suppression of blood activation and coagulation on the beads.

1. Introduction

Various materials are employed in blood-contacting implantable and extracorporeal medical devices, such as artificial hearts, artificial blood vessels, hemodialyzers and apheresis columns. Since most of those medical devices have poorly biocompatible surfaces, anticoagulants such as ethylenediaminetetraacetic acid (EDTA), hirudin, heparin, and warfarin are utilized for preventing thrombosis and embolism induced by the contact of blood with these medical devices [1]. Given the side effects of these anticoagulants, such as heparin-induced thrombocytopenia [2,3]; however, numerous efforts have been made to reduce the activation of blood in response to contact with material surfaces. Suppression of such blood activation can effectively reduce the amount of anticoagulant required. In order to improve the blood compatibility of material surfaces, a number of versatile methods have been applied. One of the most simple and important techniques is polymer coating using biocompatible polymers such as poly(ethylene glycol) [4], zwitterionic polymers [5-7], microphase-separated polymers [8,9], and poly(2-methoxyethyl acrylate) [10]. These approaches can drastically reduce the adsorption of serum proteins. Protein adsorption triggers the activation of blood cells and blood coagulation on material surfaces through

5

a complex series of events, including the activation of platelets, leukocytes, complement, and the fibrinolytic system [11]. Therefore, it has long been thought that the suppression of protein adsorption is highly important in the design of blood-compatible surfaces. Nevertheless, even today, all blood-contacting devices cause thrombosis in long-term usage. In fact, synthetic vascular grafts with inside diameters of less than 6 mm cannot be used because they are prone to early thrombotic occlusion [12]. In the case of cardiac stents, drug-eluting stents have been developed for the inhibition of endothelial cell proliferation and restenosis, but even these stents were found to be thrombogenic [13,14].

Recently, gaseous molecules such as oxygen, nitric oxide, carbon monoxide and hydrogen sulfide are reported to play important roles for numerous biological events. New strategy utilizing these gaseous molecules has been proposed. For example, polymer, which releases nitric oxide, shows high performance on the suppression of blood activation [15-18]. Interestingly, it has been revealed that blood–material interactions cause an increase in the levels of reactive oxygen species (ROS) and inflammatory cytokines, which is brought about by the activation of blood cells; this leads to blood coagulation and whole body inflammation (see Figure 1a) [19-21]. The excess ROS continuously amplify inflammation, thereby increasing the risk of

potentially life-threatening disorders [22]. Indeed, long-term hemodialysis therapy induces cardiovascular disease and atherosclerotic complications, which result in high morbidity and mortality in chronic renal failure patients [23]. However, there have been few reports with experimental evidence that ROS generation is related to inflammation in blood when in contact with the material surface, and the extent of ROS involvement in inflammation is not yet clear.

We have focused on the effect of ROS-scavenging materials in vivo and have used nitroxide radicals, such as 2,2,6,6-tetramethylpiperidine-*N*-oxyl (TEMPO), which catalytically react with ROS [24-26] and can be used as electron spin resonance (ESR) probes in vivo [27,28]. Core–shell-type polymeric micelles containing nitroxide radicals have already been developed for the treatment of oxidative stress injuries and in vivo ESR imaging [29,30]. It has been confirmed that they not only strongly scavenge ROS in vivo or in vitro but also significantly prevent oxidative stress damage in an cerebral ischemia–reperfusion injury model in rats [31], renal ischemia–reperfusion injury model in mice [32] and a neuron cell line used as a model for Alzheimer's disease [33,34], in which excess ROS is generated. In the process, we have hypothesized that ROS-scavenging characteristics play a crucial role in blood activation and coagulation when blood comes in contact with material surfaces. To validate our hypothesis, we

have designed and developed a hydrophobic nitroxide radical-containing polymer (NRP) composed of hydrophobic poly(chloromethylstyrene) (PCMS) chains in which TEMPO moieties were conjugated via condensation reaction of the chloromethyl groups in PCMS with the sodium alkolate group of 4-hydroxy-TEMPO (TEMPOL) (see Figure 1b).   In this paper, we describe the synthesis of the NRP homopolymer and its characterization in terms of blood compatibility.

2. Experimental Sections

2.1 Materials

2,2'-Azobisisobutyronitrile (AIBN; Kanto Chemical Co., Inc., Tokyo, Japan) was purified by recrystallization from methanol. Chloromethylstyrene (CMS; > 95%), which was kindly provided by Seimi Chemical Co., Ltd. (Kanagawa, Japan), was washed three times with 20% NaOH aqueous solution to remove inhibitors, washed three times with water, and dried using sodium sulfate, followed by vacuum distillation under nitrogen atmosphere (2.0 mmHg, 56°C). N,N-Dimethylformamide (DMF; Kanto Chemical Co., Inc., Tokyo, Japan) was purified by vacuum distillation under nitrogen atmosphere by a molecular sieve. Tetrahydrofuran (THF), methanol, benzene, sodium hydride, 1,4-dioxane, n-decane (Kanto Chemical Co., Inc., Tokyo, Japan), TEMPOL, hypoxanthine (HX), xanthine oxidase (XOD; Aldrich Chemical Co., Inc., USA), and 2-methyl-6-p-methoxyphenylethynylimidazopyrazinone (MPEC; ATTO Co., Inc., Tokyo, Japan), and heparin (Mochida Pharmaceutical, Tokyo, Japan) were used without further purification.

2.2 Synthesis of NRP

After 1 mmol of AIBN was weighed into a flask, the inside of the reactor was degassed and filled with nitrogen gas. The degassing–N_2–purge cycle was repeated

three times.   CMS (100 mmol; 14.2 mL), 50 mL of 1,4-dioxane, and 3 mL of n-decane

as an internal standard for gas chromatography, were then added to the flask under

nitrogen atmosphere.   Polymerization was conducted for 18 h at 65°C in an oil bath.

After the reaction, the obtained polymer was recovered three times by precipitation into

1 L of methanol, followed by freeze-drying with benzene.   The yield of the obtained

polymer was 63.2% (9.6 g).   Conversion of CMS was 61.5%, as determined by gas

chromatography.   After 20 mg of the obtained PCMS (average molecular weight [Mw]

$= 2.6 \times 10^4$, Mw/Mn = 2.1) was weighed into the flask, dry DMF (1 mL) was added to

the flask under nitrogen atmosphere.   A solution of TEMPOL in dry DMF (1 mL) was

added to a suspension of sodium hydride at molar quantity of TEMPOL in dry DMF (1

mL); the mixture was stirred for 1 min, followed by addition to the PCMS solution in

dry DMF under nitrogen atmosphere.   The mixture was stirred at room temperature for

10 h.   The feed molar ratio of TEMPOL to chloromethyl groups in the PCMS

homopolymer was systematically changed as summarized in Table 1.   Following this

reaction, the mixture was directly used for coating glass beads.

2.3 Preparation of NRP-coated beads (NRP beads)

10

Glass beads (average diameter: 200 μm) were washed by Soxhlet extraction with methanol, and glass beads (7 g) were immersed in the reaction mixture (3 mL) for 30 min, followed by vacuum drying over night.   In order to remove unreacted TEMPOL from NRP beads, Soxhlet extraction was carried out with water for 8 h.   To determine the extent of TEMPO moieties in the obtained NRP, ESR spectroscopy of the extract and X-ray photoelectron spectroscopy (XPS) of the coated glass beads were used.   In ESR measurements, the extent of the TEMPO moieties in the obtained NRP was determined by the ESR signal area of TEMPOL initially fed into the reaction (fed TEMPOL), and unreacted TEMPOL in the extract (see Table 1 and Table S1).   In XPS, the extent of TEMPO coverage of the NRP beads was calculated from the ratio of the N1s (in TEMPO) and Cl2p (chloromethyl groups in the polymer) peak areas (see Table 1 and Figure 3).   To confirm the coating of NRP on glass beads, coated substances on the glass beads were solubilized by chloroform after Soxhlet extraction and the ESR spectrum of the solubilized component in chloroform was measured.

2.4 Measurement of the amount of superoxide generated by the HX/XOD model system

The superoxide-scavenging activity of NRP was measured using MPEC as a superoxide-reactive chemiluminescence (CL) producer.   After polymer-coated beads (50 mg) were added into each well of a 96-well micro-plate, 10 μL MPEC (1 mM) in ethanol, 50 μL XOD (0.1 U/mL), and HX (0.72 mM) were added to each well, followed by the immediate measurement of CL using a microplate reader (Wallac 1420 ARVOsx Multilabel counter; Perkin–Elmer Life Sciences, Tokyo, Japan) at 37ºC for 1 min.

2.5 Animal

Male Sprague–Dawley rats (body weight, 150-250 g; age, 5-6 weeks; Charles River, Japan) were maintained in the experimental animal facilities at the University of Tsukuba.   All experiments were performed according to the Guide for the Care and Use of Laboratory Animals at the University of Tsukuba.   Animals were anesthetized initially with pentobarbital sodium (20–30 mg/kg).   Thereafter, blood (9 mL) was collected by cardiopuncture from outside the body using heparinized syringes (50 IU/mL, 1 mL), transferred to a siliconized tube, and kept on ice.   The final concentration of heparin was 5 IU/mL.

2.6 Measurement of the amount of superoxide in blood

The amount of superoxide generated by contact between blood and polymer-coated beads was measured using MPEC.   After the polymer-coated beads (50 mg) were added to each well on the 96-well micro-plate, 50 μL of MPEC (1 mM) in ethanol and 50 μL of diluted whole blood (2% w/w), which was diluted with saline, were added to each well, and the CL was immediately measured using a microplate reader at 37ºC for 10 min.

2.7 Measurement of the levels of inflammatory cytokines in plasma

After the polymer-coated beads (100 mg) were added to the siliconized tube, 50 μL of saline and 400 μL of heparinized rat whole blood were added to each tube, followed by incubation at 37ºC for 30 min with gentle rotation (1 rpm) by tube rotator (RT-5 TAITEC, Tokyo, Japan).   After incubation, plasma samples (100 μL) were obtained by centrifugation (2,000 rpm, 2 min) of the blood.   The plasma levels of tumor necrosis factor-α (TNF-α) and interleukin-1β (IL-1β) were measured using a commercially available enzyme-linked immunoassay kits for rat (Thermo Scientific Pierce Protein Research Products, Rockford, IL, USA), according to the manufacturer's instructions.

2.8 Measurement of leukocyte and platelet levels in rat whole blood

After the polymer-coated beads (100 mg) were added to the siliconized tube, 50 µL of saline and 400 µL of heparinized rat whole blood were added to each tube, followed by incubation at room temperature for 30 min with gentle rotation (1 rpm) by tube rotator. Suitable amount of coated beads was determined by the experiment of bead-weight dependency, as shown in Figure S1. After incubation, the blood samples were transferred to an EDTA-coated tube and then placed on ice until further analysis. To prepare EDTA-coated tubes, EDTA solution (1.2 mg/mL, 10 µL) in saline was added to siliconized tube, followed by then dried under reducing pressure. Blood cells in the sample were counted with a fully automatic hematology analyzer (Celltac α, MEK-6358; Nihon Kohden Co., Tokyo, Japan). Relative platelet count (%) is expressed as the value relative to that without beads under the same experimental procedures; relative leukocyte count (%) is also calculated in a similar way.

2.9 Scanning electron microscopy

The NRP-coated glass beads were incubated with heparinized rat whole blood for 30 min and rinsed with phosphate buffered saline (PBS) three times to remove weakly adhered blood cells; then, the adhered blood cells were fixed with a glutaraldehyde

solution (1.25 v/v%) in PBS at room temperature.   They were then dehydrated by

treatment with gradual ethanol/distilled water mixture from 50% to 100% ethanol in

steps of 10%.   After dehydration, the specimens were rinsed in a mixture (50/50) of

ethanol/tertiary-butyl alcohol for 15 min, followed by incubation with tertiary-butyl

alcohol twice for 15 min.   The resulting specimens were freeze-dried for 2 days and

then platinum-coated using an ion sputter coater, followed by the measurement of

scanning electron microscopy (SEM; JSM-6320F, JEOL).

2.10 Instruments

Size exclusion chromatography (SEC) was performed using TOSOH HLC-8120

equipped with TSK gel columns (Super HZ4000 and Super HZ3000) and an internal

refractive index (RI) detector.   THF with 5% (v/v) triethylamine was used as the eluent

at a flow rate of 0.35 mL/min at 40°C.   The ^{1}H NMR spectra were obtained using

chloroform-d on a JEOL EX270 spectrometer at 270 MHz.   The ^{1}H NMR spectra were

collected with the following parameters: temperature, 25°C; numbers of scan, 64.   The

ESR spectra were recorded at room temperature on a Bruker EMX-T ESR spectrometer

operating at 9.7 GHz with a 100-kHz magnetic field modulation.   The spectra were

collected with the following parameters: sweep width, 500 G; microwave power, 0.633

mW; receiver gain, 5.02×10^4; time constant, 5.120 ms; and conversion time, 10.240 ms.

Atomic concentration information was obtained by XPS (Thermo K-Alpha XPS, Thermo Fisher Scientific, West Palm Beach, FL, USA). The instrument was equipped with a monochromatic Al-Kα X-ray source ($hv = 1468.6$ eV). The XPS analysis chamber was evacuated to a pressure of 5×10^{-7} Pa before collecting the XPS spectra. Spectra were collected using an X-ray spot size of 400 μm and pass energy of 100 eV.

3. Results & discussion

3.1 Synthesis of NRP and preparation of NRP beads

The PCMS homopolymer was synthesized by classical free-radical polymerization of CMS. Figure S2 shows the SEC diagram and ^{1}H NMR spectrum of the obtained PCMS. The SEC diagram showed that the Mw and the molecular weight distribution were 26,000 and 2.1, respectively. After the polymerization, the ^{1}H NMR signal for the methylene protons of the chloromethyl group in PCMS at 4.5 ppm could still be detected in full; this indicated that any side reaction of the chloromethyl groups in PCMS can be ignored during polymerization. Stable nitroxide radicals were conjugated as side chains of the homopolymer via the condensation reaction with the sodium alkolate group of TEMPOL. In order to coat the obtained polymer onto glass beads, the beads were added to the reaction mixture; they were then dried under reducing pressure and purified using Soxhlet extraction with water in order to remove any unreacted TEMPOL. To confirm the removal of unreacted TEMPOL, aliquots of the extract were collected at several time points during the Soxhlet extraction and their ESR spectra were measured, as shown in Figure S3. Increasing ESR signal intensity was observed as a function of the washing time, with the signal intensity reaching the maximum at 7 h. To confirm the coating of the polymer on glass beads, substances

coated on the glass beads were solubilized using chloroform after the Soxhlet extraction, and the ESR spectrum of the solubilized components in chloroform was measured.   As shown in Figure 2, in contrast to the clear triplet signal of the extract after Soxhlet extraction, the ESR spectrum of the component solubilized in chloroform showed a broad signal.   Since the ESR spectra of low-molecular-weight TEMPO derivatives generally show a clear triplet signal, because of an interaction between the ^{14}N nuclei and the unpaired electron in the dilute solution, the sharp triplet signals of the extract show that only unreacted TEMPOL was successfully removed from the coated beads by Soxhlet extraction.   On the other hand, when a good solvent is used, the ESR signal of the nitroxide radical, which is present as side chains of the polymer, becomes broad owing to the spin–spin interaction of the stable radicals in the side chains [35]; the broad signal detected for the solubilized component in chloroform showed that NRP was firmly coated on the glass beads.   In addition, the NRP coating beads was confirmed by XPS.   As shown in Figure 3, the signals for nitrogen (N 1s) and chlorine (Cl 2p) in NRP and those for chlorine (Cl 2p) in the PCMS polymer were observed in conjunction with the signal for the glass beads; this shows that NRP or PCMS were tightly coated on the glass beads.   In order to determine the extent of the TEMPO moieties in the obtained NRP, the ESR and XPS data were quantitatively analyzed.   In

ESR measurements, the extent of the TEMPO moieties in the NRP was determined by

the ESR signal area of fed TEMPOL and unreacted TEMPOL in the extract, as shown in

Table S1.   Increasing the amount of fed TEMPOL results in an increase in the extent of

TEMPO in the obtained NRP.   The XPS data also show the same trend as the ESR

data; by increasing the amount of fed TEMPOL, the peak area of the N 1s signal of

TEMPO increases and the peak area of the Cl 2p signal of PCMS decreases, as shown

in Figure 3 and Table 1.   On the basis of these results, it was confirmed that the

TEMPO moieties were successfully introduced into the polymer, and NRP was firmly

coated on the glass beads.

3.2 Suppression of blood activation by NRP beads

Nitroxide radicals, in particular TEMPO derivatives, are known to not only

catalytically scavenge superoxide radicals but also scavenge carbon-centered, peroxy

radicals and hydroxyl radical [36].   In previous studies, we had developed polymeric

micelles composed of an amphiphilic block copolymer possessing TEMPO moieties as

side chains and confirmed their ROS-scavenging activity in vivo or in vitro [31-34].

Here, we first investigated whether nitroxide radicals on NRP beads can similarly

scavenge superoxide generated by the HX/XOD model system.   As shown in Figure 4,

the quantity of superoxide did not decrease in the case of PCMS-coated beads (PCMS

beads). In contrast, NRP beads decreased the levels of superoxide depending on the

TEMPO extent in the NRP beads, thus indicating that nitroxide radicals on the NRP

beads work effectively as ROS scavengers. To investigate the effect of NRP coating

on the blood activation and coagulation, we used heparinized rat whole blood.

Quantitative evaluation of the superoxide-scavenging activity of NRP beads was carried

out after placing the coated beads in contact with diluted rat whole blood, as shown in

Figure 5. The quantity of superoxide in blood gradually increased with time when

blood was in contact with PCMS beads, whereas NRP beads significantly suppressed

superoxide generation, with the result that superoxide levels did not increase.

Although it has been known that heparin interferes with leukocyte function even at

lower doses [37], excessive ROS generation was observed in the case of PCMS beads as

a control. On the other hand, NRP beads completely scavenged ROS generated by the

contact of diluted whole blood including heparin to bead surface. The dependence of

superoxide suppression on the extent of TEMPO in the polymer was then investigated.

With increasing of TEMPO extent in the NRP beads, the levels of superoxide in the

blood decreased, in a similar way to the results of the HX/XOD model system. These

results showed that ROS generation occurs in a predictable manner and that nitroxide

radicals on the beads are effective as ROS scavengers in blood. Furthermore, we investigated the effect of ROS-scavenging activity by NRP beads on the generation of inflammatory cytokines. As shown in Figure 6, placing rat whole blood in contact with PCMS beads leads to an increase in the levels of TNF-α and IL-1β in blood, whereas NRP beads significantly suppress the increase in the levels of inflammatory cytokines. These results suggest that NRP significantly inhibits the generation of inflammatory cytokines, which is induced by contact of whole blood with coated beads, in comparison with PCMS beads. This shows that the suppression of ROS generation leads to the inhibition of inflammation, which is induced by the contact of blood with foreign materials.

3.3 Suppression of blood coagulation by the NRP beads

The NRP beads were found to suppress ROS generation, which also results in the suppression of inflammatory cytokine production. In order to investigate the effect of inhibition of blood activation on blood coagulation, rat whole blood was incubated with the coated beads and the change in the number of both platelets and leukocytes was measured using a cytometer. Figure 7 shows the levels of platelets and leukocytes as a function of the extent of TEMPO in NRP beads. The numbers of both platelets and

leukocytes decreased significantly in blood after incubation of rat whole blood with

PCMS beads.   In contrast, with increases in the TEMPO extent in the polymer, this

decrease in blood levels of platelets and leukocytes was suppressed, and this finding

strongly suggested that NRP had suppressed blood coagulation.   SEM images of the

coated beads were recorded to show the coagulation of blood.   As shown in Figure 8,

high levels of blood coagulation were observed on the PCMS beads.   In contrast, the

NRP coated surfaces were smooth, and almost no coagulation was observed on the

surface.   From these results, it is clear that NRP coated surfaces can inhibit blood

coagulation.   ROS scavenging character worked effectively on the suppression of

blood cell activations. Freedman reported that NO rapidly reacts with ROS to result in

suppression of blood activation [38].   The ROS scavenging character of NRP might

influence the role of NO, which will be investigated further and will be published

elsewhere.   Here, we emphasize that this finding is, to our knowledge, the first

evidence that the use of ROS-scavenging materials as surfaces causes suppression of

inflammation and blood coagulation.   On the basis of our results, we would like to

propose that ROS-scavenging characteristics should be a key point in the design of

biomaterials such as blood-contacting surfaces.

5. Conclusion

This study has shown that NRP was successfully synthesized and coated on glass beads. When placing coated beads in contact with rat whole blood, NRP beads decreased the generation of ROS and inflammatory cytokines, thus resulting in the suppression of blood coagulation. On the basis of these results, NRP is thus anticipated to be a new blood compatible-material that attenuates the activation of blood cells and blood coagulation.

5. Acknowledgements

Figure Legends

Figure 1. Schematic illustration of (a) the mechanism of blood activation and coagulation and (b) the NRP coated surface, which can scavenge ROS and inhibit blood coagulation.

Figure 2. ESR spectra of (a) extract and (b) chloroform solution, including the solubilized component from the surface of the glass beads following Soxhlet extraction.

Figure 3. The XPS spectra of (a) NRP beads-93%; (b) NRP beads-67%; (c) NRP beads-22%; (d) PCMS beads; and (e) bare glass beads.

Figure 4. The scavenging activity of NRP against superoxide generated by the HX/XOD model system.

Figure 5. The ROS-scavenging activity of NRP against superoxide generated by placing coated beads in contact with rat whole blood (2% w/w). (a) Time-course of chemiluminescence intensity after contact with NRP beads-93% (closed square) and

PCMS beads (open square) with rat whole blood. (b) Dependence of ROS-scavenging

activity on the TEMPO extent of NRP.   (The bar graphs represent means ± SE for 6

independent experiments.)

Figure 6   Measurement of the levels of inflammatory cytokines (TNF-α and IL-1β) in

whole blood stimulated by NRP beads-93% (black bar) and PCMS beads (white bar).

(The bar graphs represent means ± SE for 6 independent experiments. *P <0.01 and

**P <0.05, Student's t-test)

Figure 7   Change in the numbers of platelets (closed square) and leukocytes (open

square) in blood as a function of the TEMPO extent of NRP. (The bar graphs represent

means ± SE for 6 independent experiments.)

Figure 8   SEM images of beads coated with (a) PCMS and (b) NRP after contact

with rat whole blood for 30 min.

Table Legend

Table 1   TEMPO extent in NRP, as determined by XPS and ESR

References:

[1] Kidane AG, Salacinski H, Tiwari A, Bruckdorfer KR, Seifalian AM. Anticoagulant and Antiplatelet Agents: Their Clinical and Device Application(s) Together with Usages to Engineer Surfaces. Biomacromolecules 2004;5:798–813.

[2] Warkentin T, Levine M, Hirsh J, Horsewood P, Roberts R, Gent M, et al. Heparin-induced thrombocytopenia in patients treated with low-molecular-weight heparin or unfractionated heparin. New Eng J Med 1995;332:1330–1335.

[3] Warkentin TE, Kelton JG, Ontario H. A 14-Year Study of Heparin-induced Thrombocytopenia. Am J Med 1996;101:502–527.

[4] Lee H, Lee J, Andrade J. Blood compatibility of polyethylene oxide surfaces. Prog Polym Sci 1995;20:1043–1079.

[5] Ishihara K, Tsuji T, Kurosaki T, Nakabayashi N. Hemocompatibility on graft copolymers composed of poly(2-methacryloxyethyl phosphorylcholine) side chain and poly(n-butyl methacrylate) backbone. J Biomed Mater Res 1994;28:225–232.

[6] Ishihara K, Aragaki R, Ueda T, Watanabe A, Nakabayashi N. Reduced thrombogenicity of polymers having phospholipid polar groups. J Biomed Mater Res 1990;24:1069–1077.

[7] Jiang Y, Rongbing B, Ling T, Jian S, Sicong L. Blood compatibility of polyurethane surface grafted copolymerization with sulfobetaine monomer. Coll Surf B: Biointerfaces 2004;36:27–33.

[8] Okano T, Nishiyama S, Shinohara I, Akaike T, Sakurai Y, Kataoka K, et al. Effect of hydrophilic and hydrophobic microdomains on mode of interaction between block polymer and blood platelets. J Biomed Mater Res 1981;15:393–402.

[9] Kikuchi A, Okano T. Nanostructured designs of biomedical materials: applications of cell sheet engineering to functional regenerative tissues and organs. J Controlled Release 2005;101:69–84.

[10] Tanaka M, Motomura T, Kawada M, Anzai T, Kasori Y, Shiroya T, et al. Blood compatible aspects of poly(2-methoxyethylacrylate) (PMEA) relationship between protein adsorption and platelet adhesion on PMEA surface. Biomaterials 2000;21:1471–1481.

[11] Anderson J, Rodriguez A, Chang D. Foreign body reaction to biomaterials. Semin Immunol 2008;20:86–100.

[12] Salacinski HJ, Tiwari A, Hamilton G, Seifalian AM. Cellular engineering of vascular bypass grafts: role of chemical coatings for enhancing endothelial cell attachment. Med Biol Eng Comput 2001;39:609–618.

[13] Mauri L, Hsieh WH, Massaro JM, Ho KK, D'Agostino R, Cutlip DE. Stent thrombosis in randomized clinical trials of drug-eluting stents. N Engl J Med 2007;356:1020–1029.

[14] Moreno R, Fernández C, Hernández R, Alfonso F, Angiolillo DJ, Sabaté M, et al. Drug-eluting stent thrombosis: results from a pooled analysis including 10 randomized studies. J Am Coll Cardiol 2005;45:954–959.

[15] Zhengrong Z, Meyerhoff ME. Preparation and characterization of polymeric coatings with combined nitric oxide release and immobilized active heparin. Biomaterials 2005;26:6506-6517.

[16] Smith D, Chakravarthy D, Pulfer S, Simmons M, Hrabie J, Citro M, Saavedra J, Davies K, Hutsell T, Mooradian D. et al. Nitric oxide-releasing polymers containing the [N(O)NO]- group. Journal of Medicinal Chemistry 1996;39:1148-1156.

[17] Major T, Brant D, Reynolds M, Bartlett R, Meyerhoff M, Handa H, et al. The attenuation of platelet and monocyte activation in a rabbit model of extracorporeal circulation by a nitric oxide releasing polymer. Biomaterials 2010; 31: 2736-2745.

[18] Reynolds M, Frost M, Meyerhoff M. Nitric oxide-releasing hydrophobic polymers: preparation, characterization, and potential biomedical applications. Free Radical Biology & Medicine 2004; 37: 926-936.

[19] Xue Y, Liu X, Sun J. PU/PTFE-stimulated monocyte-derived soluble factors induced inflammatory activation in endothelial cells. Toxicol In Vitro 2010;24:404–410.

[20] Nilsson B, Ekdahl KN, Mollnes TE, Lambris JD. The role of complement in biomaterial-induced inflammation. Mol Immunol 2007;44:82–94.

[21] Khodr B, Khalil Z. Modulation of inflammation by reactive oxygen species: implications for aging and tissue repair. Free Radic Biol Med 2001;30:1–8.

[22] Iuliano L, Colavita A, Leo R, Praticò D, Violi F. Oxygen free radicals and platelet activation. Free Radic Biol Med 1997;22:999–1006.

[23] Sarnak MJ. Cardiovascular complications in chronic kidney disease. Am J Kidney Dis 2003;41:11–17.

[24] Rachmilewitz D, Karmeli F, Okon E, Samuni A. A novel antiulcerogenic stable

radical prevents gastric mucosal lesions in rats. Gut 1994;35:1181–1188.

[25] Krishna MC, Russo A, Mitchell JB, Goldstein S, Dafni H, Samuni A. Do nitroxide antioxidants act as scavengers of O2-. or as SOD mimics? J Biol Chem 1996;271:26026–26031.

[26] Wilcox CS. Effects of tempol and redox-cycling nitroxides in models of oxidative stress. Pharmacol Ther 2010;26:119–145.

[27] Utsumi H, Yamada K, Ichikawa K, Sakai K, Kinoshita Y, Matsumoto S, et al. Simultaneous molecular imaging of redox reactions monitored by Overhauser-enhanced MRI with ^{14}N- and ^{15}N-labeled nitroxyl radicals. PNAS 2006;103:1463–1468.

[28] He G, Deng Y, Li H, Kuppusamy P, Zweier JL. EPR/NMR co-imaging for anatomic registration of free-radical images. Magn Reson Med 2002;47:571–578.

[29] Yoshitomi T, Miyamoto D, Nagasaki Y. Design of core-shell-type nanoparticles carrying stable radicals in the core. Biomacromolecules 2009;10:596–601.

[30] Yoshitomi T, Suzuki R, Mamiya T, Matsui H, Hirayama A, Nagasaki Y. pH-Sensitive radical-containing-nanoparticle (RNP) for the L-band-EPR imaging of low pH circumstances. Bioconjugate Chem 2009;20:1792–1798.

[31] Marushima A, Suzuki K, Nagasaki Y, Yoshitomi T, Toh K, Tsurushima H, et al. Newly synthesized radical-containing nanoparticles (RNP) enhance neuroprotection after cerebral ischemia-reperfusion injury. Neurosurgery 2011;68:1418–1426.

[32] Yoshitomi T, Hirayama A, Nagasaki Y. The ROS scavenging and renal protective effects of pH-responsive nitroxide radical-containing nanoparticles. Biomaterials

2011; 32: 8021–8028.

[33] Chonpathompikunlert P, Yoshitomi T, Han J, Toh K, Isoda H, Nagasaki Y. Chemical Nanotherapy-Nitroxyl Radical-containing Nanoparticle (RNP) Protects Neuroblastoma SH-SY5Y cells from Aβ-induced Oxidative Stress. Ther Deliv 2011; 2:585–597.

[34] Chonpathompikunlert P, Yoshitomi T, Han J, Isoda H, Nagasaki Y. The Use of Nitroxide Radical-containing Nanoparticles Coupled with Piperine to Protect Neuroblastoma SH-SY5Y cells from Aβ-Induced Oxidative Stress, Biomaterials 2011;32:8605–8612.

[35] Yoshida E, Tanaka T. Oxidation-induced micellization of a diblock copolymer containing stable nitroxyl radicals. Colloid Polym Sci 2006;285:135–144.

[36] Soule BP, Hyodo F, Matsumoto K, Simone NL, Cook JA, Krishna MC, et al. The chemistry and biology of nitroxide compounds. Free Radic Biol Med 2007;42:1632–1650.

[37] Peter K, Schwarz M, Conradt C, Nordt T, Moser M, Kübler W, Bode C, Heparin Inhibits Ligand Binding to the Leukocyte Integrin Mac-1 (CD11b/CD18). Circulation 1999;100:1533–1539.

[38] Freedman JE, Oxidative Stress and Platelets. Arterioscler Thromb Vasc Biol 2008; 28:s11-s16.
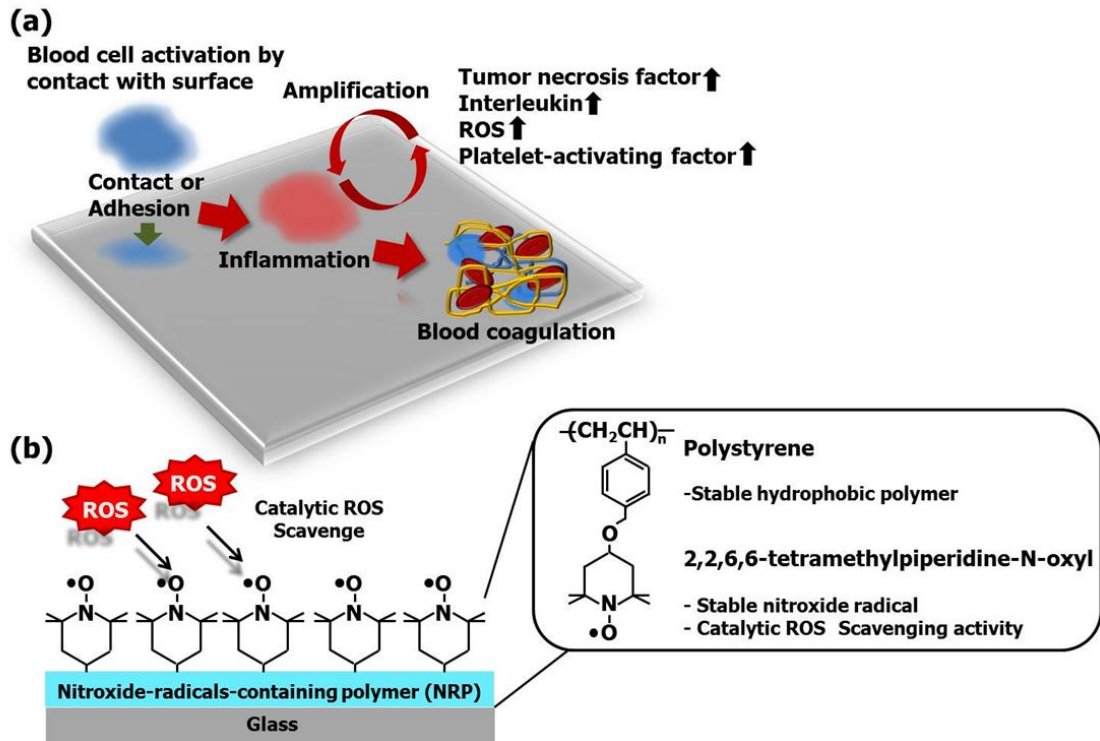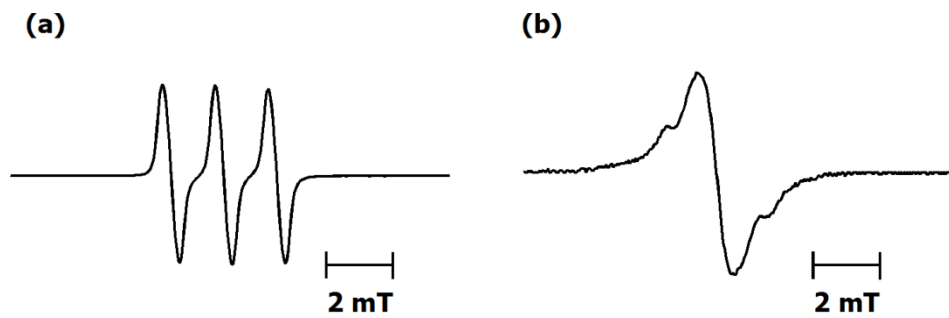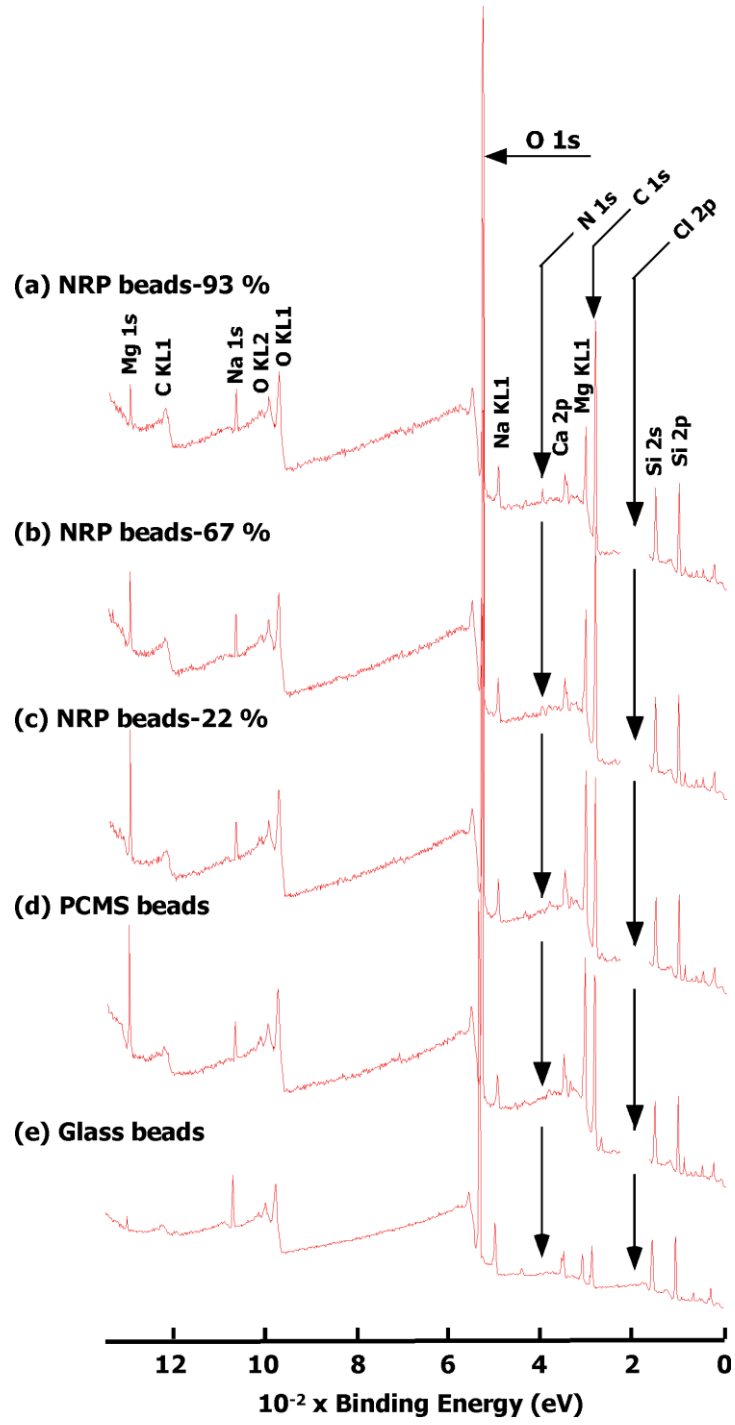
30

Figure 1.

(a)

Blood cell activation by
contact with surface

Amplification

Tumor necrosis factor ↑
Interleukin ↑
ROS ↑
Platelet-activating factor ↑

Contact or
Adhesion

Inflammation

Blood coagulation

(b)

ROS   ROS

ROS   ROS

Catalytic ROS
Scavenge

Nitroxide-radicals-containing polymer (NRP)

Glass

$-(CH_2CH)_n-$ **Polystyrene**

-Stable hydrophobic polymer

2,2,6,6-tetramethylpiperidine-N-oxyl

- Stable nitroxide radical
- Catalytic ROS Scavenging activity

Figure 2.

(a)

2 mT

(b)

2 mT

Figure 3.

Figure 4.

Figure 5.
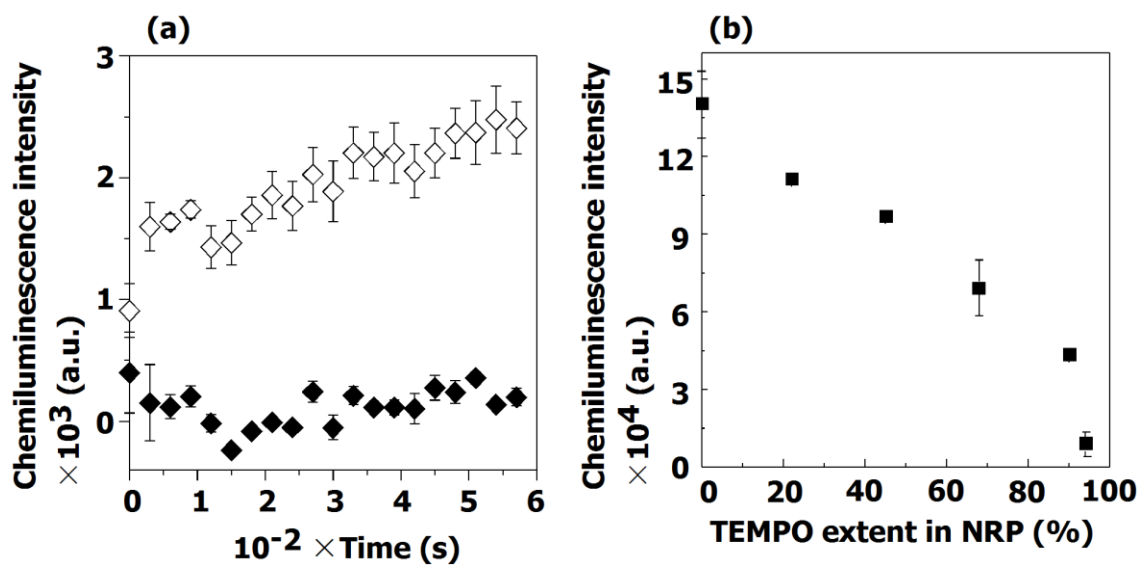
Figure 6

Figure 7

Figure 8

(a)

(b)
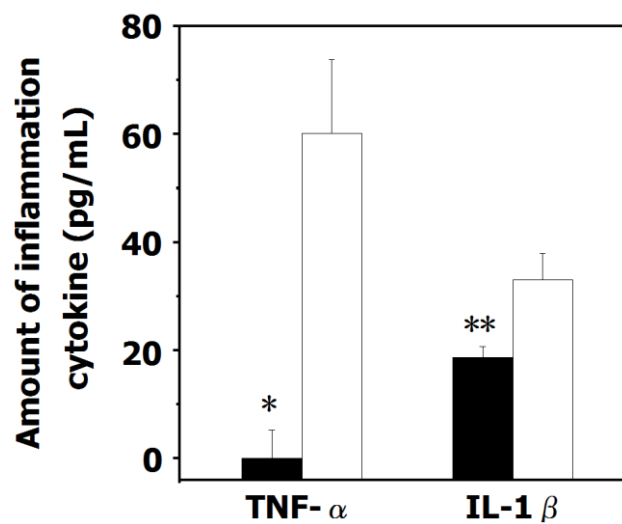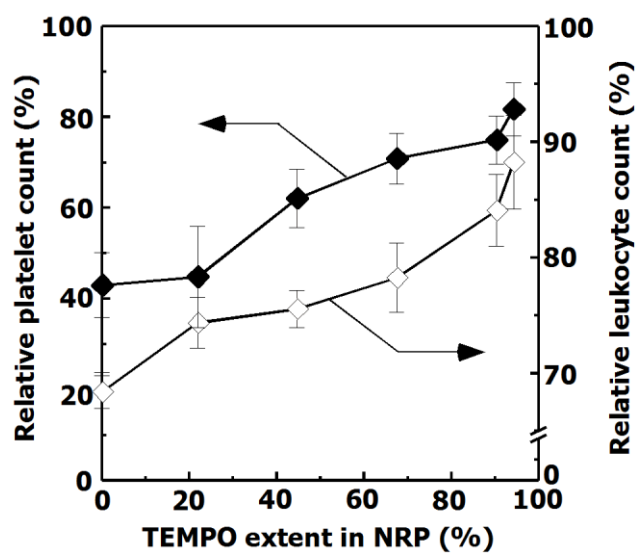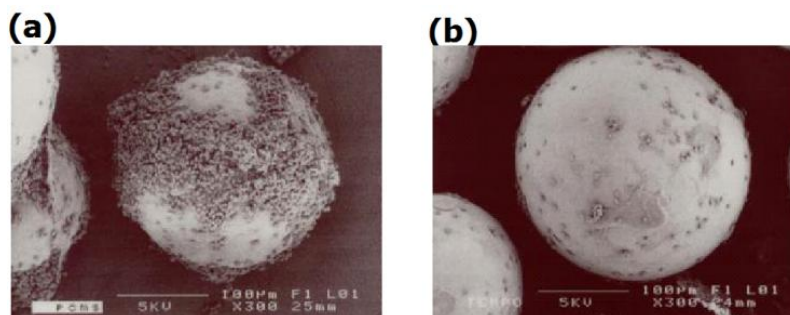
Table 1

*Sample	**Feed ratio of T/CM	% Peak area ratio		TEMPO content in NRP (%)	
		Cl 2p	N 1s	***XPS	ESR
Glass beads	-	0.18	0.11	-	-
PCMS beads	0	2.27	0.18	-	-
NRP beads-22 %	0.23	1.09	0.36	24.8	22.0
NRP beads-45 %	0.47	0.64	0.58	47.5	45.1
NRP beads-67 %	0.70	0.48	0.95	66.4	67.3
NRP beads-90 %	0.92	0.41	1.08	72.5	89.6
NRP beads-93 %	1.85	0.13	1.24	90.5	92.9

  * Percentage in NRP beads are written using the value of TEMPO content in NRP determined by ESR.
  ** Feed ratio of T/CM means the feed molar ratio of TEMPOL to chloromethyl groups in PCMS homopolymer
***The values of TEMPO content in XPS data were calculated by below fomula.

$$\text{TEMPO content (\%)} = \frac{\text{peak area of nitrogen (N 1s)}}{\text{peak area of nitrogen (N 1s)} + \text{peak area of chlorine (Cl 2p)}} \times 100$$

Graphical abstract

Nitroxide radical containing polymer (NRP) effectively scavenge reactive oxygen species (ROS) to suppress activation and adsorption of blood cells on the surface